Numerical study of subcooled boiling phenomena using a component analysis code, CUPID

Ba-Ro Lee [a], Yeon-Gun Lee [a*]
[a]*Department of Nuclear and Energy Engineering, Jeju National University, #66 Jejudahakno, Jeju-si, Jeju, KOREA*
[*]*Corresponding author: yeongun2@jejunu.ac.kr*

1. Introduction

Subcooled boiling is encountered in many industrial applications in the power and process industry. In nuclear reactors, under certain conditions, subcooled boiling may be encountered in the core. The movement of bubbles generated by subcooled boiling affect the heat transfer characteristics and the pressure drop of the system. Thus some experimental and analysis using safety codes works have been already performed by previous investigators.[1 ~ 7] It has been reported that the existing safety analysis codes have some weaknesses in predicting subcooled boiling phenomena at low-pressure conditions. Thus, it is required to improve the predictive capability of thermal-hydraulic analysis codes on subcooled boiling phenomenon at low-pressure conditions. In this study, a couple of subcooled boiling experiments at high- (> 10 bar) and low-pressure (near atmospheric pressure) conditions are analyzed using a three-dimensional thermal-hydraulic component code, CUPID. And then the analysis results compared with the results using MARS-KS code.

2. CUPID code

The CUPID code was developed by the Korea Atomic Energy Research Institute in 2010, which was motivated from practical needs for the realistic simulation of two-phase flows in nuclear reactor components.

2.1 Governing equations.

The governing equations of the two-fluid, three-field model used in the CUPID code are similar to those of the time-averaged two-fluid model derived by Ishii and Hibiki.[8] The continuity, momentum, and energy equations for the k-phase are given by

$$\frac{\partial}{\partial t}(\alpha_k \rho_k) + \nabla \cdot (\alpha_k \rho_k U_k) = \Gamma_k \tag{1}$$

$$\frac{\partial}{\partial t}(\alpha_k \rho_k U_k) + \nabla \cdot (\alpha_k \rho_k U_k U_k) = -\alpha_k \nabla P + \nabla \cdot [\alpha_k (\tau_k + \tau_k^T)] + \alpha_k \rho_k g + P \nabla \alpha_k + M_k^{mass} + M_k^{drag} + M_k^{VM} + M_k^{non-drag} \tag{2}$$

$$\frac{\partial}{\partial t}[\alpha_k \rho_k e_k] + \nabla \cdot (\alpha_k \rho_k e_k U_k) = -\nabla \cdot (\alpha_k q_k) + \nabla \alpha_k \tau_k : \nabla U_k - P \frac{\partial}{\partial t} \alpha_k - P \nabla \cdot (\alpha_k U_k) + I_k + Q'''_k \tag{3}$$

where α_k, ρ_k, U_k, P_k, Γ_k, I_k are the k-phase volume fraction, density, velocity, pressure, interface mass transfer rate and energy transfer rate. And M_k represents the interfacial momentum transfer due to mass exchange, drag force, virtual mass and non-drag forces.

To consider a turbulence effect, the k-ε turbulence model was also implemented. The classical lift force, wall lubrication force by Antal et al.[9] and turbulent dispersion force derived by Lopez de Bertodano[10] were implemented as non-drag forces.

2.2 Heat partitioning model

The CUPID code calculate the amount of vapor generation using the wall heat partitioning model. The mechanism of a heat transfer from the wall consist of the quenching heat flux q''_q, evaporation heat flux q''_e, and convection heat flux q''_c as following:

$$q''_q = \left(\frac{2}{\sqrt{\pi}} \sqrt{t_w k_l \rho_l C_{Pl}\, f} \right) A_{bub} \left(T_w - T_l \right) \tag{4}$$

$$q''_e = N'' f \left(\frac{6}{\pi} d_{Bd}^3 \right) \rho_g h_{lg} \tag{5}$$

$$q''_c = St \rho_l C_{Pl} U_l \left(T_w - T_l \right) \left(1 - A_{bub} \right) \tag{6}$$

$$A_{bub} = \min \left[1, N'' K \left(\frac{\pi d_{Bd}^2}{4} \right) \right]$$

The prediction of the heat partitioning model depends greatly on the submodels for the active nuclear site density, the bubble departure diameter, the bubble departure frequency, and the k-factor. The default models for these main parameters adopted in the CUPID code are summarized in Table 1.

3. Analysis of subcooled boiling experiments

In this study, total 4 experiments are analyzed using CUPID code(Christensen, Bartolomey, Zeitoun, and SUBO experiments). Christensen[1] and Bartolomey[2] tested subcooled boiling at high pressure condition(> 10 bar). Zeitoun[3] and SUBO[4] conducted subcooled boiling test in a low pressure condition(near atmospheric pressure).

Table 1: Heat partitioning model of CUPID code

Parameter	Model
Active nucleate site density	Cole(1960) $N'' = \left[185\left(T_w - T_{sat}\right)\right]^{1.805}$
Bubble departure diameter	Cole and Rohsenow(1969) $d_{Bd} = 1.5\times10^{-4}\sqrt{\frac{\sigma}{g\Delta\rho}}\,Ja^{*5/4}$ $Ja^{*} = \rho_l C_{Pl} T_{sat} / \rho_g h_{lg}$
Bubble departure frequency	Cole(1960) $f = \sqrt{\frac{4g\Delta\rho}{3d_{Bd}\rho_l}}$
K-factor	4

3.1 Christensen's and Bartolomey's tests.

The test section of Christensen's subcooled boiling experiment is a rectangular channel with a cross section of 11.1 x 44.4 mm. The heated length of the test section is 1270 mm. And the test section of Bartolomey's tests is a cylindrical channel of 24 mm in test section diameter. The heated length of the test section is 2000 mm. The experimental conditions of Christensen's and Bartolomey's tests analyzed using CUPID and MARS-KS code are summarized in Table 2 and 3.

Table 2: Test conditions of Christensen's experiments selected for CUPID and MARS-KS code analyses

Name	Pressure (bar)	Power (kW)	Mass flux (kg/m^{2}s)	Temperature (K)	Inlet subcooling (K)
Case 1	27.6	30	646.9	493.7	8.7
Case 2	68.9	70	807.7	545.9	12.1

Table 3: Test conditions of Bartolomey's experiments selected for CUPID and MARS-KS code analyses

Name	Pressure (bar)	Heat flux (kW/m^2)	Mass flux (kg/m^{2}s)	Temperature (K)	Inlet subcooling (K)
Case 3	30	380	890	483.15	25.0
Case 4	45	380	890	504.15	24.0

The number of mesh is optimized through a series of preliminary runs to find the minimum mesh number over which the void fraction no longer varies ($<10^{-4}$) as the node is refined. So the total mesh number of Christensen's geometry is 1024 x 25. And Bartolomey's geometry mesh number is 1049 x 40. The steady solution could be obtained at 10 seconds.

The calculated void fraction is compared to the measured ones in Fig. 1 ~ 4. The x-axis of those figures indicates the height of test section. In case 1, the average void fraction error between CUPID code and measurement is 0.040, and the average void fraction error between the MARS-KS code and measurement is 0.033. In case 2, the average void fraction error between the CUPID code and measurement is 0.025, and the average void fraction error between MARS-KS code and measurement is 0.054. And the CUPID code's average void fraction error is 0.022 by case 3 and 4. Those show that the CUPID code is good agreement with measurement data.

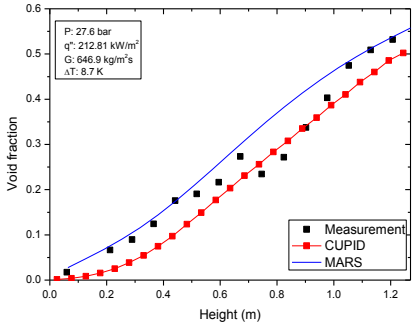

Fig. 1 Comparison of CUPID and MARS-KS for case 1

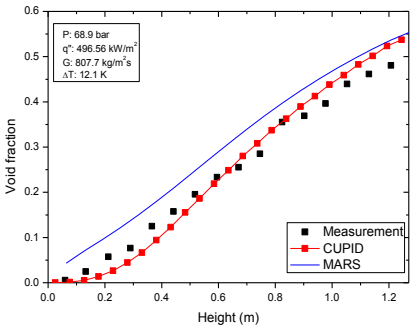

Fig. 2 Comparison of CUPID and MARS-KS for case 2

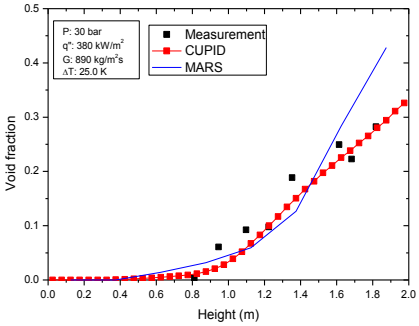

Fig. 3 Comparison of CUPID and MARS-KS for case 3

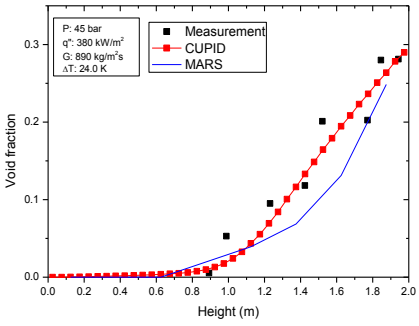

Fig. 4 Comparison of CUPID and MARS-KS for case 4

3.2 Zeitoun's tests.

The test section of Zeitoun's experiments a vertically arranged annulus with an in-direct heater rod at channel center. The inner diameter of the test section is 25.4 mm, and the outer diameter of the heater rod is 12.7 mm. The heated length of the test section is 306 mm. The test section for the boiling heat transfer was short in length and local bubble parameters were not provided. The mesh number of CUPID code is set to 658 x 10. The experimental conditions analyzed using CUPID code are summarized in Table 4.

Table 4: Test conditions of Zeitoun's experiments selected for CUPID and MARS-KS code analyses

Name	Pressure (bar)	Heat flux (kW/m^2)	Mass flux (kg/m^2s)	Temperature (K)	Inlet subcooling (K)
Case 5	1.23	478.5	283.1	358.97	19.7
Case 6	1.14	210	188.9	365.09	11.4

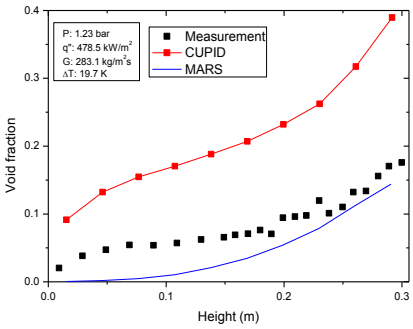

Fig. 5 Comparison of CUPID and MARS-KS for case 5

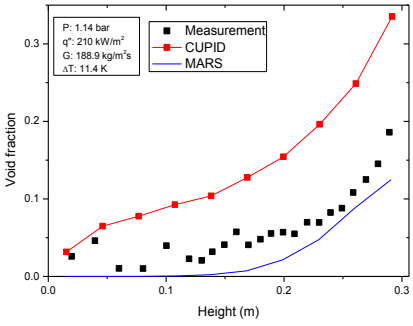

Fig. 6 Comparison of CUPID and MARS-KS for case 6

The MARS-KS code average void fraction error is 0.032 and 0.011. It is seen that the results gotten by the MARS-KS code and the data of measurement are in good agreement. But the CUPID analysis result is different with the result at high-pressure condition (Christensen and Bartolomey). All case shows that the CUPID code is higher void fraction prediction than experimental data. The CUPID code average void fraction error is near 0.1. The maximum measurement data is 0.2 or less, it was confirmed that a fairly large error.

3.3 SUBO tests.

The test section of SUBO experiments similar to Zeitoun's test section. But except for geometry shape, the height of test section and test conditions is different. The inner diameter of the test section is 9.98 mm, and the outer diameter of the heater rod is 35.5 mm. The heated length of the test section is 3883 mm. SUBO experiment was measured radial void fraction using optical probes. The mesh number of CUPID code is set to 290 x 100. The experimental conditions analyzed using CUPID code are summarized in Table 5

Table 5: Test conditions of SUBO experiments selected for CUPID and MARS-KS code analyses

Name	Pressure (bar)	Heat flux (kW/m^2)	Mass flux (kg/m^2s)	Temperature (K)	Inlet subcooling (K)
Case 7	1.616	473.7	1124.7	374.65	17.8
Case 8	1.551	373.6	1122.9	374.25	17.2

The calculated void fraction is compared to the measured one in Figs. 7 ~ 10. The result of CUPID code analysis is similar to the result of CUPID code of Zeitoun's test. All case and all point are show high prediction of void fraction. And then radial void fraction distribution is not match to measurement data. Average void fraction error is 0.087 and 0.111. So the sensitivity analysis of submodels in the heat partitioning model was performed to evaluate the parametric effect of major factors on the void fraction distribution and to find the optimized sets of submodels for low-pressure conditions.

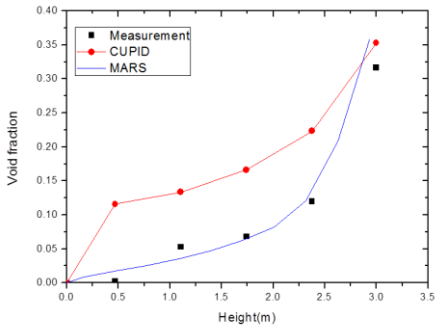

Fig. 7 Comparison of CUPID and experimental data for case 7(axial void fraction)

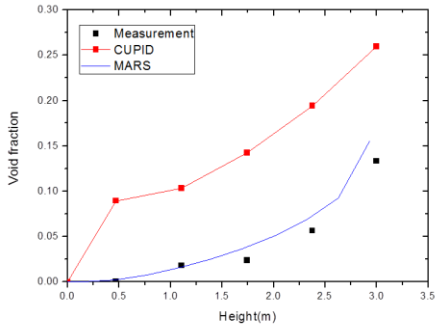

Fig. 8 Comparison of CUPID and experimental data for case 8(axial void fraction)

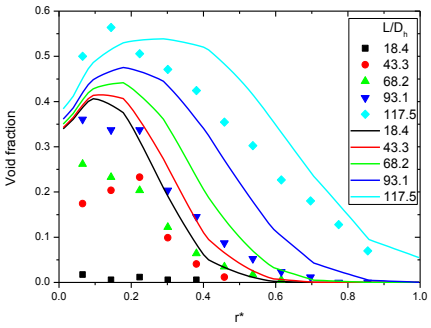

Fig. 9 Comparison of CUPID and experimental data for case 7(radial void fraction)

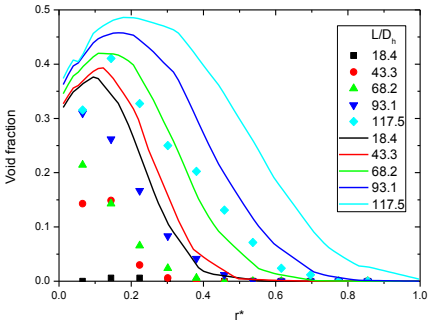

Fig. 10 Comparison of CUPID and experimental data for case 8(radial void fraction)

4. Sensitivity analysis of CUPID code

In order to improve the prediction accuracy of the void fraction, we did the sensitivity analysis of submodels in heat partitioning model. Main parameters whose effects are evaluated include the active nucleate site density, N'', the bubble departure diameter, d_{Bd}, the bubble departure frequency, f, and the K-factor, K. In this paper, we tested 4 models of the active nucleate site density and 3 models of bubble departure diameter. The sensitivity test on the bubble departure frequency and K-factor is not conducted because CUPID code does not support other models. The submodels selected for sensitivity analysis of subcooled boiling at low pressure conditions are listed in Table 6.

Table 6: Conditions of submodels selected for sensitivity analysis

Name	Active nucleate site density	Bubble departure diameter	Bubble departure frequency	K-factor
Default	Cole	Cole and Rohsenow	Cole	4
M_case1	Cole	Tolubinsky		
M_case2	Lemmert and Chwala	Cole and Rohsenow		
M_case3	Hibiki	Tolubinsky		
M_case4	Kocamustafaogullari and Ishii	Fritz		

The calculated void fractions using each set of submodels are compared to experimental data in Fig. 11. The average void fraction error and RMS(Root mean square) of each case are shown in Table 7.

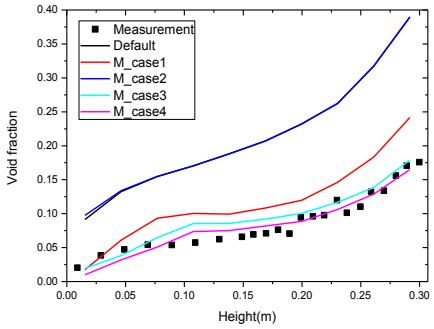

Fig. 11 Sensitivity analysis result of case 5

Table 7: Conditions of submodels selected for sensitivity analysis

	Default	M_case1	M_case2	M_case3	M_case4
Avg. error	0.128	0.035	0.128	0.012	0.011
RMS	0.137	0.039	0.137	0.015	0.012

It was selected submodels of M_case4. Because analyses result are the lowest error deviations with measurement data. The selected submodels are shown in Table 8. Kocamustafaogullari and Ishii have correlated the cumulative nucleation site density reported by various investigators for water boiling on a variety of surfaces at pressures varying from 1 to 198 bars.[15] And then, case 5 ~ 8 are reanalysis using submodels of M_case 4. The calculated void fraction is compared the default CUPID code model to the modified CUPID code model in Figs. 12 ~ 17.

In case 5 and 6, the CUPID code average void fraction error was reduced from 0.081 to 0.011 and 0.128 to 0.024, respectively. It is seen that the results gotten by the modified CUPID code and the data of measurement are in good agreement. And case 7 and 8, average void fraction error was reduced from 0.087 to

0.039 and 0.111 to 0.014, respectively. But the radial void fraction distribution is not match to experimental data. The radial void fraction distribution affected to bubble mean diameter, lift force coefficient, wall lubrication force coefficient and turbulent dispersion force coefficient. Thus, we will try to radial void fraction distribution by sensitivity analysis.

Table 8: The selected submodels of CUPID code

Parameter	Model
Active nucleate site density	Kocamustafaogullari and Ishii(1983) $N'' = D_m^2 / n^*$ $n^* = F(\rho^*) R_c^{*-4.4}$ $R_c^* = R_c / (D_m / 2)$ $\rho^* = \frac{\Delta\rho}{\rho_g}$ $F(\rho^*) = 2.157 \times 10^{-7} \rho^{*-3.2} (1 + 0.0049\rho^*)^{4.13}$ $R_c = \frac{2\sigma T_{sat}}{\rho_g h_{lg} (T_w - T_{sat})}$ $D_m = 0.0012 \rho^{*0.9} d_{Bd.F}$ $d_{Bd.F} = 0.0208\theta \sqrt{\frac{\sigma}{g\Delta\rho}}$: Bubble departure diameter of Fritz
Bubble departure diameter	Fritz(1935) $d_{Bd} = 0.0208\theta \sqrt{\frac{\sigma}{g\Delta\rho}}$
Bubble departure frequency	Cole(1960) $f = \sqrt{\frac{4g\Delta\rho}{3d_{Bd}\rho_l}}$
K-factor	4

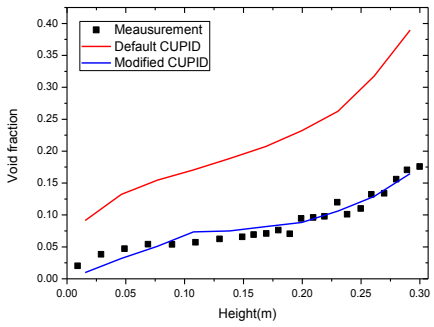

Fig. 12 Comparison of default CUPID and modified CUPID for case 5

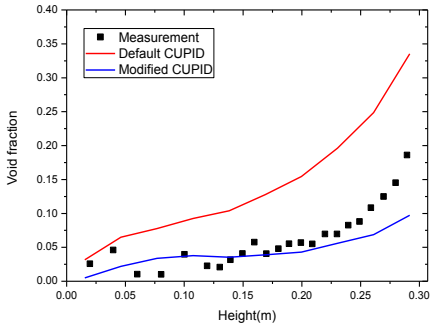

Fig. 13 Comparison of default CUPID and modified CUPID for case 6

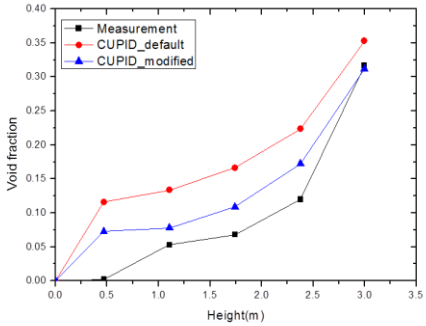

Fig. 14 Comparison of CUPID and experimental data for case 7(axial void fraction)

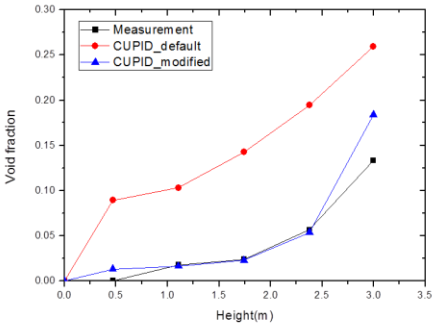

Fig. 15 Comparison of CUPID and experimental data for case 8(axial void fraction)

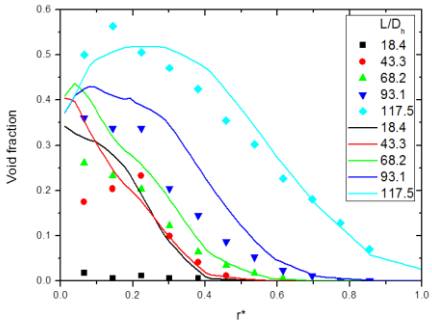

Fig. 16 Comparison of CUPID and experimental data for case 7(radial void fraction)

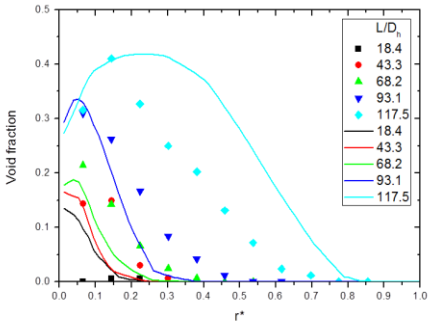

Fig. 17 Comparison of CUPID and experimental data for case 8(radial void fraction)

5. Conclusions

Subcooled boiling experiments at high- and low-pressure conditions are analyzed using a three-dimensional thermal-hydraulic component code, CUPID. The predictions of the CUPID code shows good agreement with Christenses's data and Bartolomey's data obtained at high pressure conditions. However at low pressure condition, the CUPID code generally is overestimated prediction of the void fraction.

Thus, we did selected submodels in the heat partitioning model by sensitivity analysis. Selected submodels of M_case 4 are Kocamustafaogullari and Ishii correlation model of active nucleate site density, N'' and Fritz correlation model of bubble departure diameter, d_{Bd}. And then, case 5 ~ 8 are reanalysis using submodels of M_case 4. The calculated void fraction is compared the default CUPID code model to the modified CUPID code model. As a result, average void fraction error was reduced from 0.081 to 0.011 and 0.128 to 0.024, 0.087 to 0.039, 0.111 to 0.014, respectively. But the radial void fraction distribution is still not match to experimental data.

In further work, we will try to match the radial void fraction distribution by sensitivity analysis. And then, comparison of experimental data generated Jeju National University boiling test section and CUPID code.

ACKNOWLEDGMENTS

This research was supported by Basic Science Research Program through the National Research Foundation of Korea(NRF) funded by the Ministry of Education. (No. NRF-2010-002007)

REFERENCES

[1] H. Christensen, Power-to-void transfer functions, ANL-6385, Argonne National Laboratory, Argonne, USA, 1961.
[2] C. C. Bartolomey and V. M. Chanturiya, Experimental study of true void fraction when boiling subcooled water in vertical tubes, Thermal Engng, 14, pp. 123-128, 1967.
[3] O. Zeitoun and M. Shoukri, Axial void fraction profile in low pressure subcooled flow boiling, Int. J. Heat Mass Transfer, 40, pp. 869-879, 1997.
[4] R. Situ, T. Hibiki, X. Sun, Y. Mi and M. Ishii, Axial interfacial area transport of subcooled boiling flow in an internally heated annulus, Experiments in Fluids, 37, pp.589-603, 2004.
[5] B. J. Yun, B. U. Bae, D. J. Euh, G. C. Park and C. -H. Song, Characteristic of the local bubble parameters of a subcooled boiling flow in an annulus, Nuclear Engineering and Design, 240, pp.2295-2303, 2010.
[6] B. Koncar, I. Kljenak and B. Mavko, Modelling of local two-phase flow parameters in upward subcooled flow boiling at low pressure, Int. J. Heat Mass Transfer, 47, pp. 1499-1513, 2004.
[7] J. Y. Tu and G. H. Yeoh, On numerical modeling of low-pressure subcooled boiling flows, Int. J. Heat Mass Transfer, 45, pp. 1197-1209, 2002.
[8] M. Ishii and T. Hibiki, Thermo-fluid dynamics of two-phase flow, Springer, 2006.
[9] S. P. Antal, R T. Lahey and J. E. Flaherty, Analysis of phase distribution in fully developed laminar bubbly two-phase flow, Int. J. of Multiphase Flow, 7, p.635, 1991.
[10] M. Lopez de Bertodano, Turbulent bubbly two-phase flow in a triangular duct, Ph. D., Thesis, Rensselaer Polytechnic Institute, Troy, NY, 1992.
[11] R. Cole, Photographic study of boiling in region of critical heat flux, AIChE Journal, 6, pp.533-542, 1960.
[12] R. Cole and W. Rohsenow, Correlation of bubble departure diameters for boiling of saturated liquids, Chem. Eng. Prog., 65, pp.211-213, 1969.
[13] V. I. Tolubinsky and D. M. Kostanchuk, Vapor bubbles growth rate and heat transfer intensity at subcooled water boiling, Proc. 4th Int Heat Transf Conf, Paris, France, pp.B-2.8, 1970.
[14] M. Lemmert and J. M. Chwala, Influence of flow velocity on surface boiling heat transfer coefficient, In: Hahne, E., Grigull, U. (Eds.), Heat Transfer in Boiling, Academic Press and Hemisphere, 1977.
[15] G. Kocamustafaogullari and M. Ishii, Interfacial area and nucleation site density in boiling systems, Int. J. Heat Mass Transfer, 26, pp.1377-1387, 1983.
[16] W. Fritz, Maximum volume of vapor bubbles, Phys. Z. 36, pp.379-384, 1935.
[17] T. Hibiki and M. Ishii, Active nucleation site density in boiling systems, Int. J. Heat Mass Transfer, 46, pp.2587-2601, 2003.